Sensing Urban Poverty: From the Perspective of Human Perception-based Greenery and Open-space Landscapes

Yuan Meng; Man Sing Wong;

Abstract: Greenery and open spaces play significant roles in environmentally sustainable societies, providing urban ecosystem services and economic benefits that reduce urban poverty. Current urban poverty research has solely focused on top-down observations or direct human exposure to greenery and open spaces and has failed to sense landscape characteristics, including occupation and inequality, representing urban poverty social attributes. This paper demonstrates the potential to better understand certain social characteristics, including occupation and inequality between urban greenery and open spaces and to further investigate their relationship with urban poverty. Percentage and aggregation indicators are proposed based on street view images to estimate the occupation and inequality between human perception-based greenery and open spaces. The relationship between human perception and urban poverty is accordingly analysed using geographically weighted regression (GWR). The GWR model results attain an R-squared value of 0.667 and further reveal that percentage of green perception and aggregation of open space perception are negatively related to urban poverty, while percentage of open space perception and aggregation of greenery perception are positively correlated to urban poverty in most areas. This implication suggests that greenery and open spaces can be sufficiently organised to help reduce urban poverty.

Keywords: Human Perception; Greenery; Open Space; Landscape; Urban Poverty; Street View

1. Introduction

Urban poverty refers to low-level living conditions in terms of income, housing, public facilities, education and social activities and is considered one of the important issues in facilitating city organisation and decision making (Klasen, 2000; Noble et al., 2010). Traditional approaches for measuring urban poverty are commonly based on socioeconomic situations. The use of census data and numerous urban poverty indices has been proposed, including the index of multiple deprivations (IMD) proposed by Knox and Pinch (2014), the general deprivation index (GDI) proposed by Langlois and Kitchen (2001) and the multidimensional poverty index established by Alkire and Santos (2010). These measures accurately depict socioeconomic variations to quantify urban poverty, but the impacts of the physical environment are ignored.

Remotely sensed images enable physical environment monitoring and depict the overall view of urban settlements reflecting urban poverty. On the one hand, much

research has attempted to extract characteristics including colours, textures, spectra and shapes from high-resolution images to establish indicators that quantify urban poverty (Liu et al., 2019; Wang et al., 2019a). On the other hand, night-time light images, which are proven to be correlated with human activities, have been considered for estimating the degree of deprivation (Elvidge et al., 2009). These studies promote the determination of the spatial distribution of deprived areas from the perspective of the overall physical environment. However, few of these studies examine the configurations of specific physical elements such as greenery and open spaces, and thus, they fail to provide detailed urban environment information to help reduce urban poverty.

In fact, urban greenery and open spaces have long been recognised as some of the vital components in physical environmental landscapes (Kabisch and Haase, 2014; Schroeder and Cannon, 1983). Considering their contributions to the urban environment and socioeconomic conditions, including air purification (Jim and Chen, 2008), urban heat island effect mitigation (Weng et al., 2004; Zhu et al., 2017), urban climate investigation (Oke, 2002), urban function management (Xing and Meng, 2018; Yuen et al., 2019), physical and mental health improvement (Ho et al., 2019; Lee and Maheswaran, 2011), urban crime elimination (Wolfe and Mennis, 2012) and sustainable development (Chen and Li, 2018), urban greenery and open spaces can potentially improve multiple living conditions.

Currently, various studies have focused on the correlations between urban poverty and different perspectives of greenery or open spaces. Li et al. (2019) applied vector park data from local governments and investigated how deprived communities interact with urban greenery accessibility. Li et al. (2015) utilised Google Street View (GSV) to detect the spatial distribution of residential street greenery and further analysed its relationship with the socioeconomic conditions of residents. Zhang et al. (2018) employed street-level images to segment greenery and open spaces and investigate the connection between them and socioeconomic conditions. From the above research, evidence indicates that urban greenery and open spaces are significantly related to the degree of deprivation at the regional scale.

Despite promising results on the correlations of urban poverty and greenery and open spaces, limitations still exist. As physical environments are commonly depicted through remotely sensed images and vector-format local government data, boundaries of ground surfaces, including greenery, are extracted from overhead views, and thus, the vertical dimensions of urban greenery and open spaces perceived by humans on site are not considered (Chen et al., 2014; Liu et al., 2017). On the other hand, although street view images enable the depiction of human exposure to greenery and open spaces, state-of-the-art research mainly focuses on quantifying visual perception of street-level landscapes (Helbich et al., 2019; Stubbings et al., 2019; Wang et al., 2019b; Yin and Wang, 2016) and fails to depict the social attributes of greenery and open-space landscapes such as occupation and inequality. Clearly, a knowledge gap

exists between the perception of greenery and open-space landscapes and urban poverty characterisation.

To overcome these constraints, this study proposes a novel framework to depict the social characteristics of urban greenery and open spaces, including occupation and inequality, and to further analyse their relationship with urban poverty. Adopting Tianhe District in Guangzhou as a case study, this research evaluates the hypothesis that the perceived greenery and open spaces are represented by greenery and sky segments, respectively, in street view images (Tang and Long, 2018), and quantifies urban poverty using the modified IMD by Yuan and Wu (2014). On this basis, this study further answers the following questions:

(1) How can we effectively estimate the occupation and inequality between human perception-based greenery and open spaces reflecting the social attributes of urban poverty?

(2) Are human perception-based greenery and open spaces highly correlated with the degree of urban poverty?

The remainder of this paper is organised as follows. Section 2 introduces the study area and experimental data used in this study. Section 3 illustrates the proposed framework, including human perception-based greenery and open-space landscape descriptions and the relationship analysis of these aspects with urban poverty. In Section 4, we present the greenery, open-space landscape and quantification results and how these aspects are related to urban poverty. Section 5 examines the differences between top-down- and human perception-based landscapes and the detailed relationship between human perception-based greenery and open spaces and urban poverty. Section 6 concludes this study.

2. Study Area and Data

2.1 Study Area

As one of the eleven districts in Guangzhou, Guangdong Province, Tianhe District was selected as the study area, as shown in Figure 1. Tianhe District has developed rapidly in recent decades and has become one of the commercial and cultural centres of Guangzhou. Thus, Tianhe has the advantages of having been provided with public resources and target area-based regeneration policies. On the other hand, unbalanced development still occurs in this area. With different urban landscapes, the neighbourhoods in Tianhe range from impoverished to affluent areas.

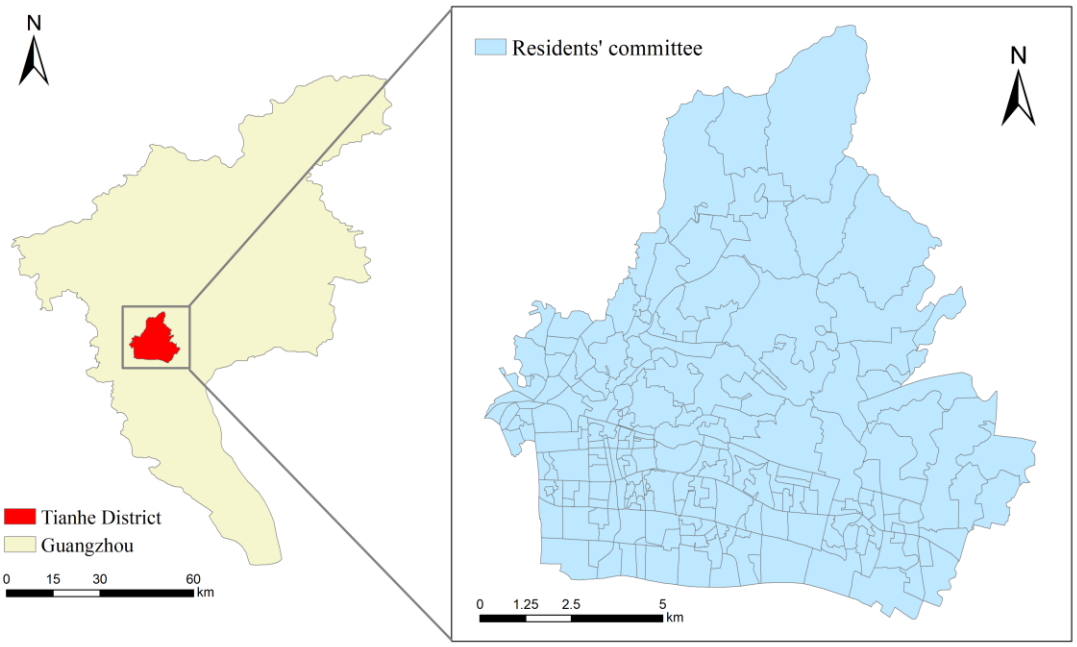

Figure 1. Spatial distribution of the study area and street view images.

2.2 Data

2.2.1 Road networks

Road networks were collected from Baidu Map (http://lbsyun.baidu.com). Roads including primary roads, secondary roads and highways, with the length of 977.61 km in total. In particular, only secondary roads were utilized with the length of 654.25 km, because landscapes near secondary roads can be reflected in detail.

2.2.2 Street View Images

Street view images were also collected from Baidu Map for data consistence (http://quanjing.baidu.com/#/). Street view locations were selected homogeneously across the road network at intervals of 100 metres. Specifically, images along four headings were collected at each location including headings of 90°, 180°, 270° and 360°. As a result, 3664 locations and 14656 street view images were obtained. After we removed primary and highway view images, 1987 locations and 7948 street view images along secondary roads were acquired.

2.2.3 Index of Multiple Deprivations

Index of Multiple Deprivations (IMD) is utilised to evaluate the degree of poverty. In this study, we followed IMD in Guangzhou calculated by Yuan and Wu (2014), which uses Chinese population census data (fifth population census) as references to measures urban poverty in terms of five aspects, including income,

employment, education, housing and health, in each residents' committee. In particular, 1) the evaluation of income includes the percentage of industrial workers and lower social-services workers in total employees, as well as percentage of female-headed families; 2) employment indicates the percentage of unemployment over 15 years old; 3) education includes percentage of people who are between 6 and 14 years old and not attending school, people with lower education attainments over 15 years old, as well as percentage of people leaving school without diploma; 4) housing mainly describes percentage of households in overcrowding conditions and without clean water, shower, clean energy or toilet; 5) health measures the ratio of disability, percentage of people in a permanent injury, illness, or physical or mental condition. As shown in Figure 2, high IMD values represent impoverished areas, while low IMD values indicate affluent regions.

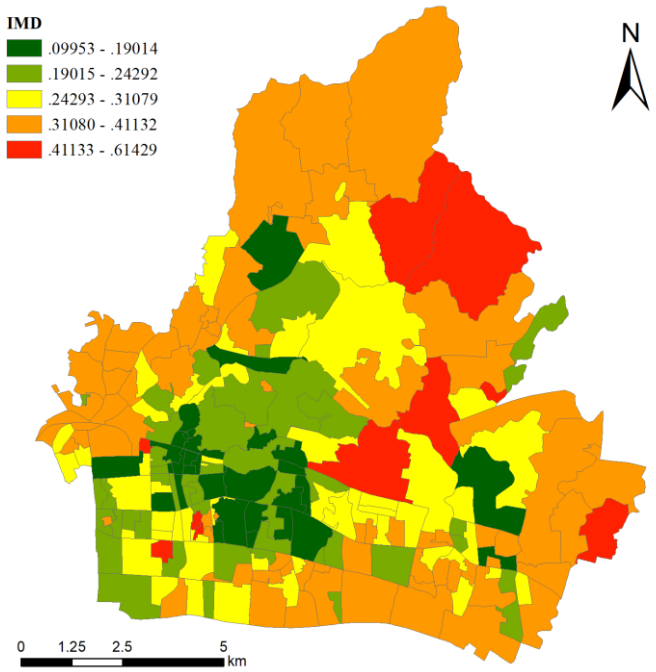

Figure 2. Spatial distribution of the IMD for quantifying urban poverty.

3. Methodology

3.1 Overview

An overall framework is proposed in Figure 3. First, image segmentation is proposed using pyramid scene parsing network (PSPNet) for extracting greenery and sky segments from street view images. Then, inverse distance weighting (IDW) is applied for identifying perception-based greenery and open-space landscapes from independent street view images. Based on the aforementioned, four landscape indicators are established, including greenery and open-space perception percentages

and aggregations. Details are provided in Section 3.2. Finally, geographically weighted regression (GWR) is utilised to analyse the relationship between human perception-based greenery and open-space landscapes and urban poverty. Details are in Section 3.3.

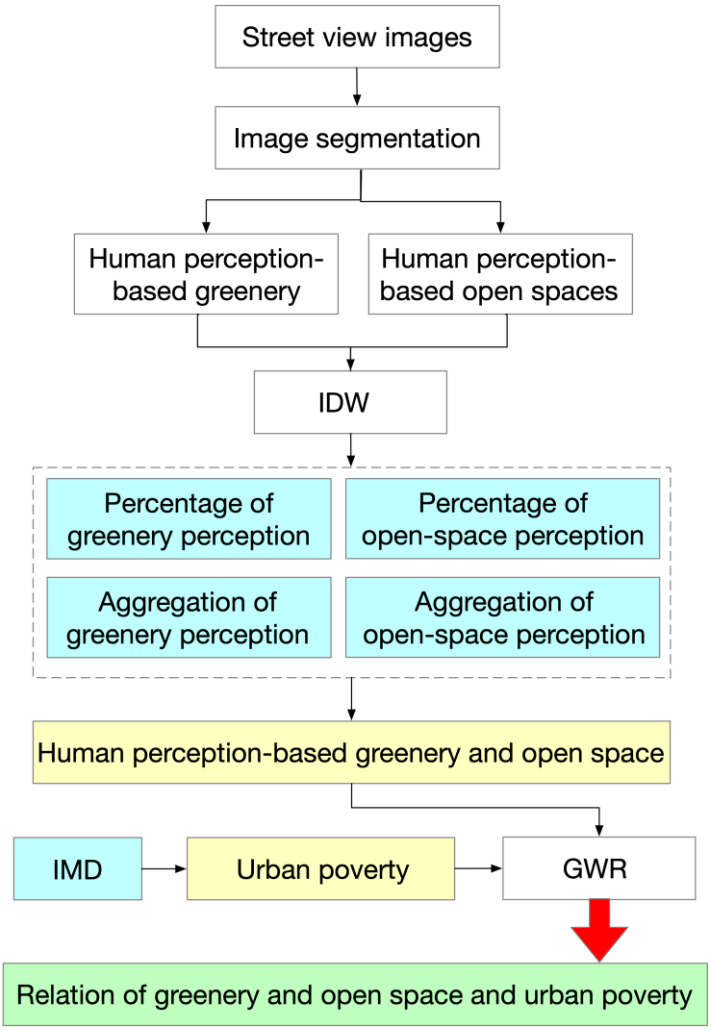

Figure 3. The overall framework.

3.2 Human Perception-based Greenery and Open-space Landscape Description

The descriptions of human perception-based greenery and open-space landscapes are based on two assumptions. First, the locations of street view images are considered accessible places, and thus, the views in these images are regarded as human-perceived location views. Second, indicators that describe greenery and open-space landscapes should depict continuous landscape characteristics in each residential area instead of individual street view places. Accordingly, in this section, deep learning is utilised to segment greenery and open spaces from street view images, and landscape indicators are proposed to depict greenery and open-space landscape characteristics.

3.2.1 Street View Image Segmentation Using Deep Learning

Image segmentation aims to recognise independent objects and depict boundaries from a single image, which is accomplished by labelling each image pixel a particular category. Thus, greenery and open spaces can be extracted from images by detecting greenery and sky pixels, respectively.

As shown in Figure 4, at each location, street view images from headings of 90°, 180°, 270° and 360° are considered for human perception. Then, different objects in these street view images are automatically labelled, including buildings, sky, greenery, and cars, by applying the pyramid scene parsing network (PSPNet) architecture (Zhao et al., 2017). Model training relies on the ADE20K dataset, and this model can reach an accuracy of 79.70% for classifying 150 categories (Zhou et al., 2017).

Based on the above, greenery and open spaces are segmented from each classified street view image. Both greenery and open spaces are calculated based on pixels. Accordingly, human perception-based greenery and open spaces can be measured as follows:

$$P_{i,greenery} = \sum_{j=1}^{4} Pixel_{j,greenery} \quad (1)$$

$$P_{i,open} = \sum_{j=1}^{4} Pixel_{j,sky} \quad (2)$$

where $P_{i,greenery}$ and $P_{i,open}$ are the total pixels recognised as greenery and open spaces, respectively, at the *i*th location, and $P_{j,greenery}$ and $P_{j,sky}$ are the greenery and sky pixels, respectively, in the *j*th street view heading.

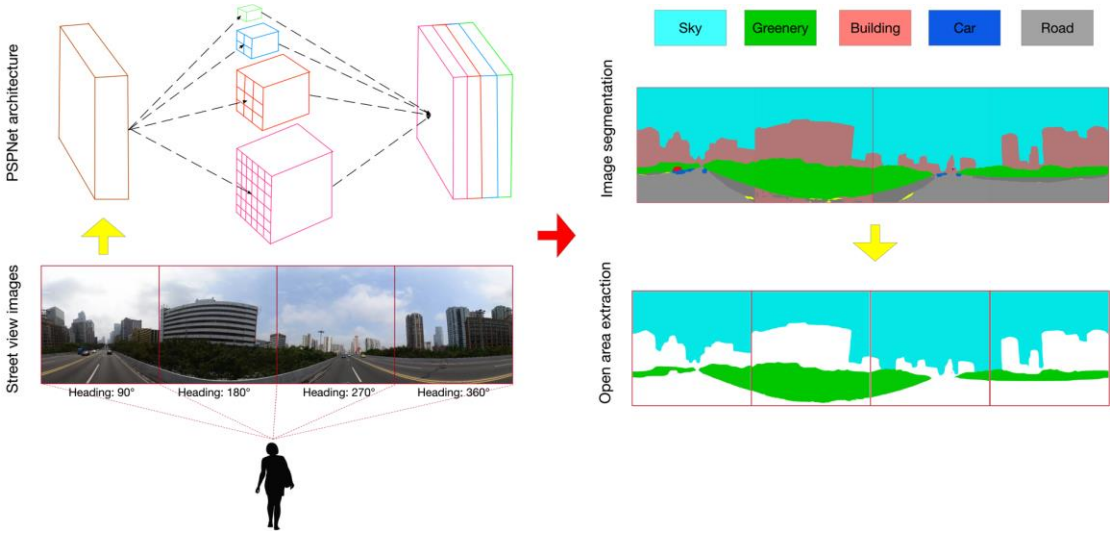

Figure 4. The workflow of street view image segmentation for human perception.

3.2.2 Greenery and Open-Space Landscape Indicators

Since human-perceived views that are closer to each other exhibit more notable correlations and similarities, independent greenery and open spaces segments from street view images at each location can be utilised to generate continuous greenery and open-space landscapes. Thus, the IDW method, which has been applied as a means of interpolation in many fields (Bartier and Keller, 1996; Chen, 2012; Zimmerman et al., 1999), is proposed to estimate the continuous occupation of greenery and open spaces based on the human-perceived views of street view images:

$$z_{Greenery} = \frac{\sum_{i=1}^{N} P_{i,greenery} \cdot d_i^{-n}}{\sum_{i=1}^{N} d_i^{-n}} \quad (3)$$

$$z_{Open} = \frac{\sum_{i=1}^{N} P_{i,Open} \cdot d_i^{-n}}{\sum_{i=1}^{N} d_i^{-n}} \quad (4)$$

where z_{Green} and z_{Open} are the estimation values of greenery and open spaces based on the *i*th location, d_i is the distance between the estimated and variable locations, and *N* and *n* are the total locations and the coefficient to be estimated, respectively.

Based on the estimated greenery and open spaces, each area is characterised by its corresponding occupation and inequality indicators.

3.2.2.1 Occupation of Greenery and Open Spaces

To quantify the occupation of greenery and open spaces, the percentages of greenery and open-space perception are utilised, respectively, which quantify the regions that people can perceive within an area. These measures define the total area occupied by human-perceived greenery and open spaces, respectively. Instead of independent street views, these indicators provide an overview of human-perceived greenery and open spaces with respect to a continuous landscape and further help examine how living conditions related to greenery and open spaces affect resident deprivation.

With regard to each area, the percentages of greenery and open-space perception are defined as follows:

$$Percentage_{greenery} = \frac{\sum_{i=1}^{N} z_{i,Greenery}}{\sum_{i=1}^{N} P_{i,all}} \quad (5)$$

$$Percentage_{open} = \frac{\sum_{i=1}^{N} z_{i,Open}}{\sum_{i=1}^{N} P_{i,all}} \quad (6)$$

where $P_{i,all}$ is calculated as:

$$P_{i,all} = \sum_{j=1}^{4} Pixel_{j,all} \quad (7)$$

where $P_{i,all}$ and $Pixel_{j,all}$ are the total pixels at the *i*th location and all pixels in the *j*th street view heading, respectively, $Percentage_{greenery}$ is the percentage of greenery perception, $Percentage_{open}$ is the percentage of open-space perception, and *N* is the total number of pixels within each area.

198

199 3.2.2.2 Inequality Between Greenery and Open Spaces

200 In terms of measuring the inequality between greenery and open spaces, the
201 greenery and open-space perception aggregations are considered for representing
202 unequal greenery and open-space distributions. In particular, the degree of
203 aggregation is quantified based on the cumulative differences between the greenery or
204 open-space perception proportion and the total perception proportion. The following
205 indicators are proposed:

$$Aggregation_{greenery} = \sum_{i=1}^{N} \left(\frac{z_{i,Greenery}}{\sum_{i=1}^{N} z_{i,Greenery}} - \frac{P_{i,all}}{\sum_{i=1}^{N} P_{i,all}} \right)^2 \quad (8)$$

$$Aggregation_{Open} = \sum_{i=1}^{N} \left(\frac{z_{i,Open}}{\sum_{i=1}^{N} z_{i,Open}} - \frac{P_{i,all}}{\sum_{i=1}^{N} P_{i,all}} \right)^2 \quad (9)$$

206 where $Aggregation_{greenery}$ and $Aggregation_{Open}$ are the aggregations of
207 greenery and open-space perception, respectively. High values indicate a high degree
208 of inequality and variability.

209 *3.3 Relationship Analysis Using GWR*

210 To analyse the relationship between human perception-based greenery and
211 open-space landscapes and urban poverty, the GWR model, which spatially extends
212 traditional linear regression, is applied. Compared with other spatial modelling
213 methods, GWR is designed to analyse regressions for all locations by estimating local
214 parameters among numerous variables (Brunsdon et al., 1996). Specifically, GWR
215 estimates a local coefficient for the *i*th location:

$$y_i = \sum_{j=0}^{j=n} \beta_{ij} * x_{ij} + \varepsilon_i \quad (10)$$

216 where y_i is the dependent variable at the *i*th location, x_{ij} are the independent
217 variables, β_{ij} is the coefficient of the *j*th independent variable at the *i*th location, and
218 ε_i is the error term. Based on the aforementioned, indicators including greenery and
219 open-space perception percentages and aggregations are adopted as independent
220 variables, and the IMD quantifying urban poverty is considered the dependent
221 variable.

222 **4. Results**

223 *4.1 Greenery and Open Spaces in Street View Images*

224 By proposing the PSPNet architecture for image segmentation, greenery and open
225 spaces were extracted from street view images. Figure 5 shows the human
226 perception-based greenery and open spaces extracted from three locations.

Considering the four headings of 90°, 180°, 270° and 360°, street view images were merged to capture the surrounding environment at each location. Based on visual inspection, the proposed PSPNet model can accurately delineate the boundaries among different objects and precisely identify greenery and open spaces from street view images. In addition, it should be noted that there are places where the greenery is obstructed by walls and not accessible (as shown in Figure 5(1)), and the greenery can solely be completely viewed in top-down observations. A detailed discussion is provided in Section 5.

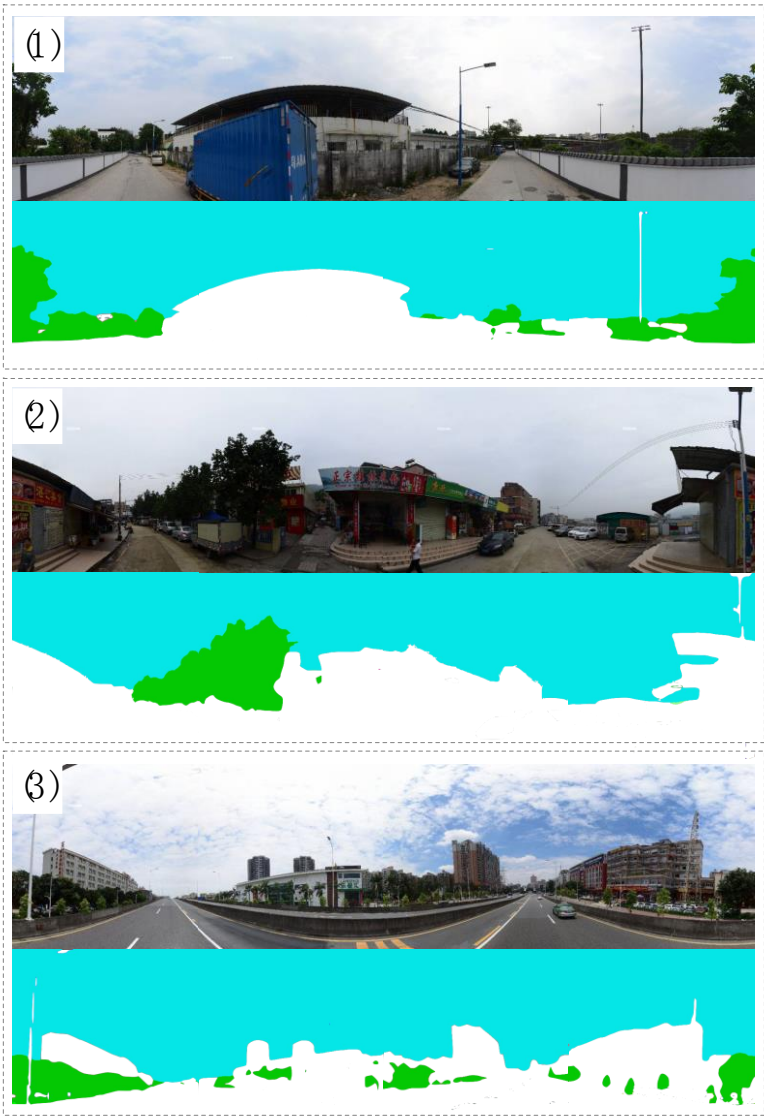

Figure 5. Examples of greenery and open-space delineations from street view images.

Following the delineation of greenery and open spaces, 7948 street view images at 1987 locations along secondary roads were utilised to identify greenery and open spaces. The pixels in an image of the same category (greenery or sky) at the same location were summed. Figure 6(a) and (b) display the human perception-based greenery and open spaces at each location, respectively. Based on visual inspection,

the human perception-based greenery in western Tianhe District is much larger than that in eastern Tianhe District, while the human perception-based open space exhibits the opposite distribution, namely, eastern Tianhe District has more open spaces than western Tianhe District.

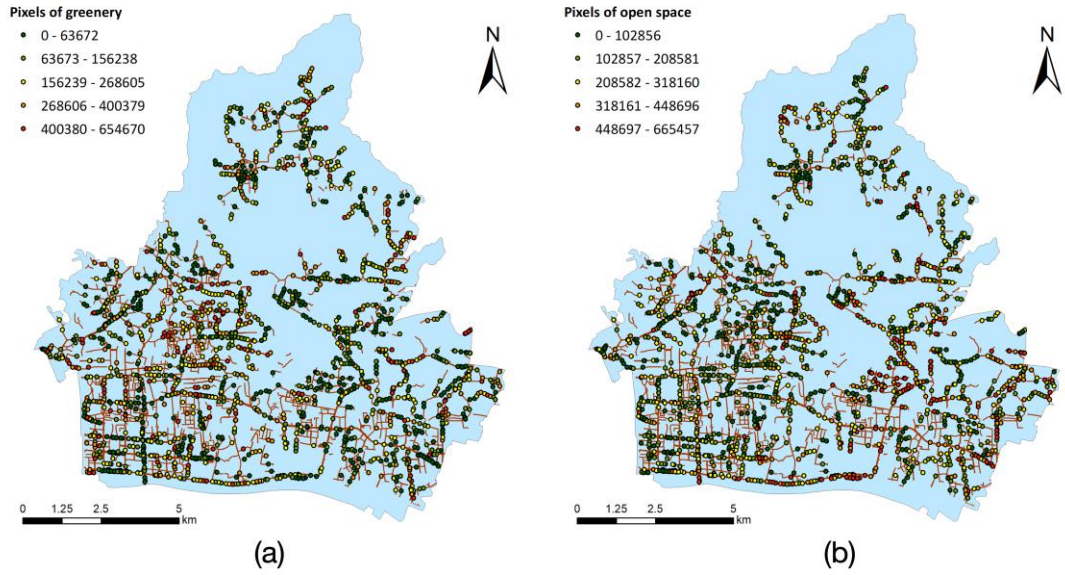

Figure 6. Pixels in street view images for representing human perception-based greenery and open spaces. (a) Greenery pixels; (b) open-space pixels.

4.2 Human Perception-based Greenery and Open-space Landscapes

To generate continuous human perception-based greenery and open-space landscapes from the images of independent locations, both greenery and open-space pixels were considered. We determined the IDW cell size as 60 metres to avoid the situation whereby each cell contains multiple street view locations and images. On this basis, the spatial distribution of the IDW greenery and open-space results are shown in Figure 7(a) and (b), respectively. These figures correspond to the visualised greenery and open spaces in Figure 6(a) and (b), respectively, and further indicate the potential distribution of greenery and open spaces at non-image locations.

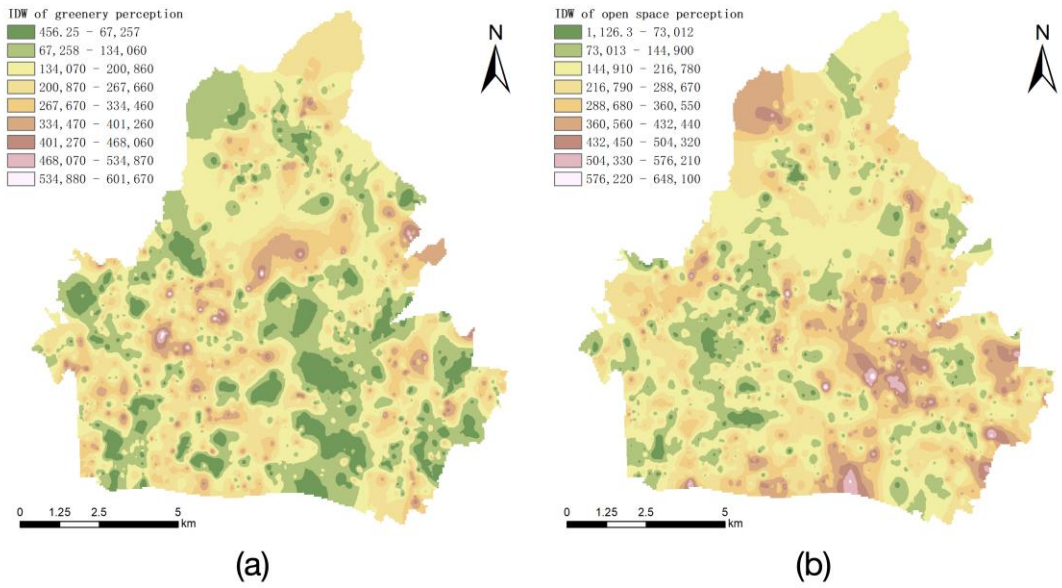

Figure 7. Spatial distribution of the IDW results. (a) IDW greenery perception results; (b) IDW open-space perception results.

According to the continuous greenery and open-space landscapes generated via IDW, four indicators, including greenery and open-space perception percentages and aggregations, were analysed to determine the greenery and open-space landscape characteristics. Figure 8(a)-(d) reveal that the proposed landscape indicators were calculated within each area. Both the greenery and open-space perception percentages exhibit homogeneous patterns in Tianhe District. Moreover, the greenery and open-space perception aggregations show similar distribution patterns, with low values in the northeast region. This indicates that northeast Tianhe District possesses more equal and invariable patterns of human perception-based greenery and open spaces compared to the other regions.

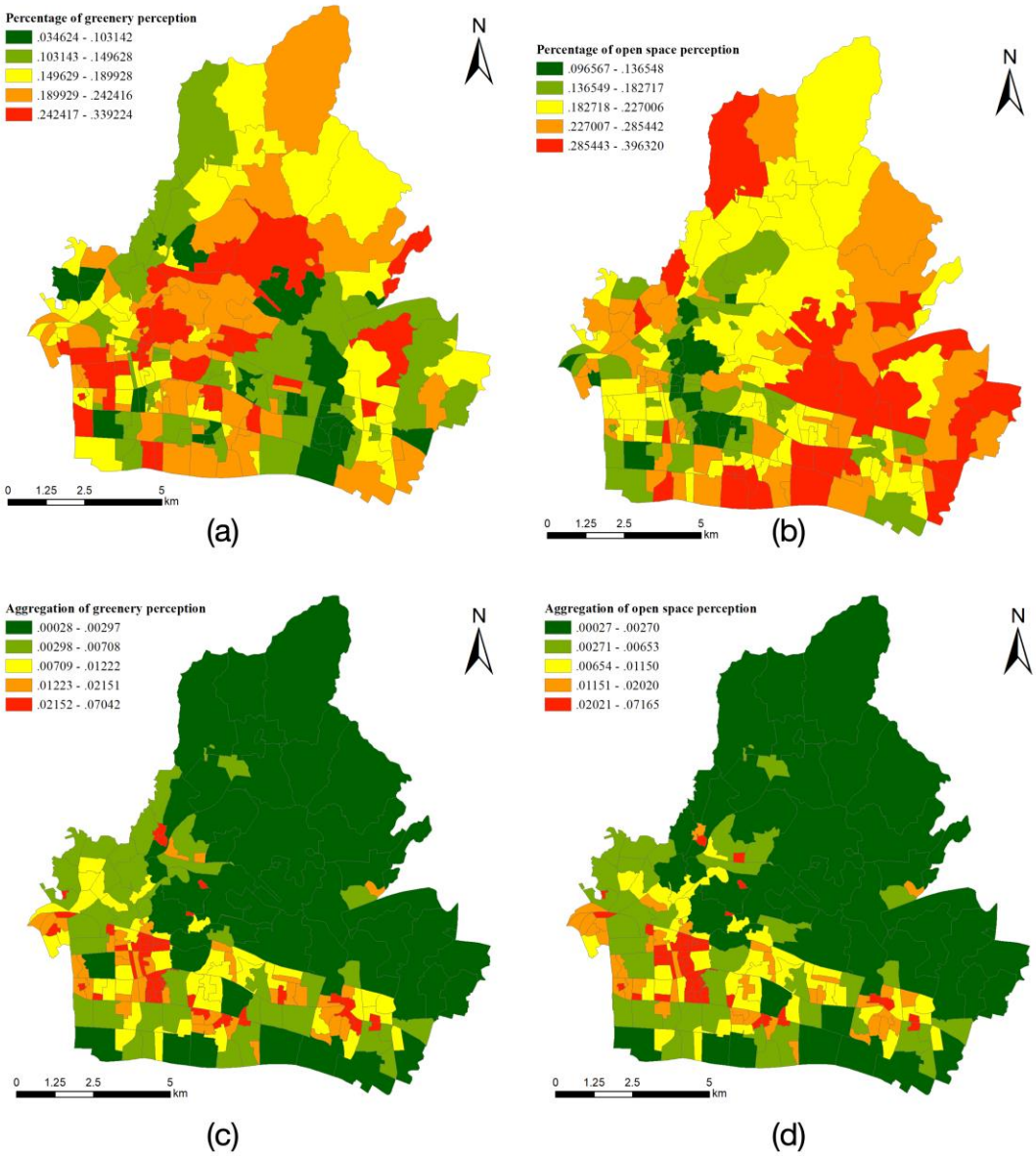

Figure 8. Spatial distribution of the human perception-based greenery and open-space landscape indicators. (a) Percentage of greenery perception; (b) percentage of open-space perception; (c) aggregation of greenery perception; (d) aggregation of open-space perception.

4.3 Relationship Between Human Perception-based Greenery and Open Spaces and Urban Poverty

Based on the quantification of human perception-based greenery and open-space landscapes, we examined the relationship between greenery and open-space landscapes and urban poverty using the GWR model. The descriptive statistics of both the independent and dependent variables were summarised in Table 1. In particular, the independent variables including greenery and open-space perception percentages and aggregations range from 0-1. The maximum greenery and open-space perception percentages are 0.3392 and 0.3963, respectively, while the minimum percentages are 0.0346 and 0.0966, respectively. In addition, both the greenery and open-space

perception aggregations range from 0.0003 to 0.07. The descriptive statistics of these indicators indicate that, from the perspective of human perception at the street level, the occupation of greenery and open spaces is relatively lower than that of built-up areas such as buildings. In addition, the aggregation values represent similar variation degrees of the inequality between greenery and open spaces among the different residential areas. This indicates that based on street views, both greenery and open spaces occupy relatively low proportions in each area compared with built-up areas. Greenery and open spaces also exhibit similar unequal distributions among the different areas, with mean aggregations of 0.0129 and 0.0122, respectively.

Table 1. Descriptive statistics of the variables in GWR.

Variables		Minimum	Maximum	Mean	Standard Deviation
Independent variables	Percentage of greenery perception	0.0346	0.3392	0.1761	0.0620
	Percentage of open-space perception	0.0966	0.3963	0.2152	0.0596
	Aggregation of greenery perception	0.0003	0.0704	0.0129	0.0118
	Aggregation of open-space perception	0.0003	0.0716	0.0122	0.0119
Dependent variables	IMD	0.0995	0.6143	0.2847	0.0858

We implemented the GWR model by determining the number of neighbours. Specifically, the number of neighbours was selected based on the following criteria. First, low Akaike's Information Criterion (AICc) and R-squared values should be lower in the fitted GWR model. Second, GWR residuals are supposed to be randomly distributed. According to the above criteria, the selected neighbours and statistical results are listed in Table 2. Based on the AICc and R-squared values, the GWR models with 20 and 30 neighbours attained a better performance than the other models. However, the GWR model with 20 neighbours has a z-score of -1.88, which is below -1.65, thus revealing a disperse rather than a random distribution. Accordingly, the GWR model with 30 neighbours is selected as the best-fitted model.

Table 2. Different numbers of neighbours in the GWR models and statistical results.

Number of neighbours	AICc	R-squared	Moran's I	Z-score	P-value
20	18.599	0.722	-0.045	-1.88	0.06
30	**95.058**	**0.667**	**-0.027**	**-1.002**	**0.316**
40	174.175	0.604	-0.012	-0.306	0.76
50	250.891	0.53	0.001	0.308	0.759
60	326.399	0.512	0.014	0.888	0.374
70	383.59	0.482	0.027	1.506	0.132
80	416.229	0.437	0.039	2.094	0.036
90	449	0.395	0.049	2.527	0.016
100	448.299	0.372	0.055	2.841	0.004

Based on the above results, the GWR coefficient results of the greenery and open-space perception percentages and aggregations are displayed in Figures 9(a)-(d). The relationship between the greenery and open-space landscape indicators and IMD is spatially inconsistent. The positive influence of these indicators is the strongest in the areas marked in red, while the areas marked in blue indicate negative correlations among the greenery and open spaces and the IMD. In particular, the impact of greenery perception in Figure 9(a) indicates that a negative trend is observed in the central and east areas in correlations between the open-space perception and degree of urban poverty. Figure 9(b) reveals that the areas in the central and north region exhibit notable positive. Figure 9(c) shows that most areas reflect positive correlations between the greenery perception aggregation and the IMD. Moreover, in Figure 9(d), most areas excluded central ones show negative trends between the open-space perception aggregation and the IMD.

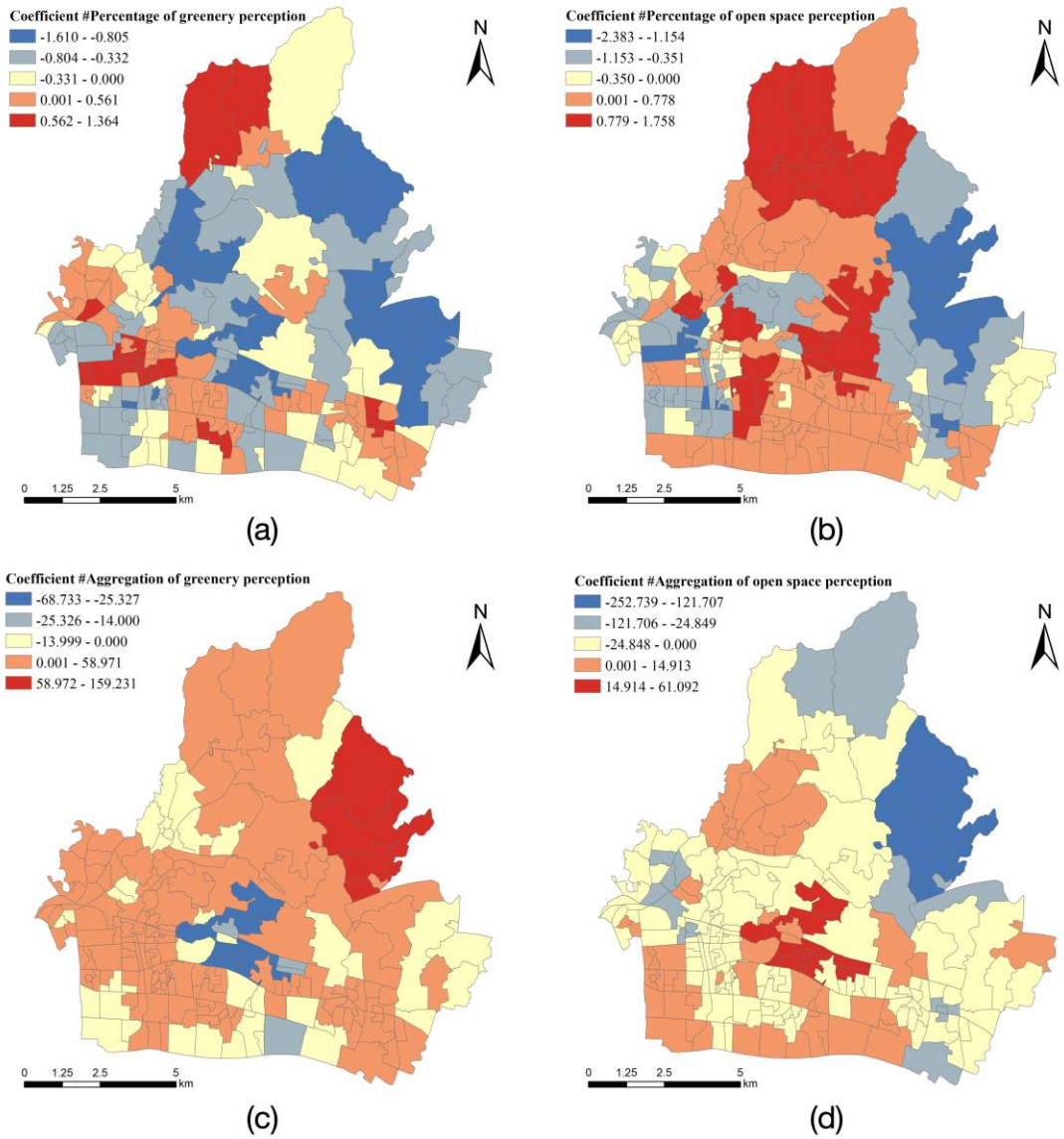

Figure 9. GWR coefficient results. (a) Percentage of greenery perception; (b) percentage of open-space perception; (c) aggregation of greenery perception; (d) aggregation of open-space perception.

The local R-squared values in Figure 10(a) indicate that the variation in greenery and open-space landscape indicators explains 0.017 to 0.828 of the variability in the IMD. In particular, the areas marked with darker colours have higher local R-squared values and are mostly located in the northwest area, while the areas marked with lighter colours have lower local R-squared values and are distributed in the southeast region. Moreover, the GWR model performance is represented by the standard residuals, revealing any spatial correlation issues. Specifically, the standard residuals usually range from -1.96 to 1.96, i.e., within the 95% confidence level. Since the standard residuals depicted in Figure 10(b) are within the acceptable range, we can conclude that the GWR model is suitable to illustrate the correlation among greenery and open-space landscapes and urban poverty.

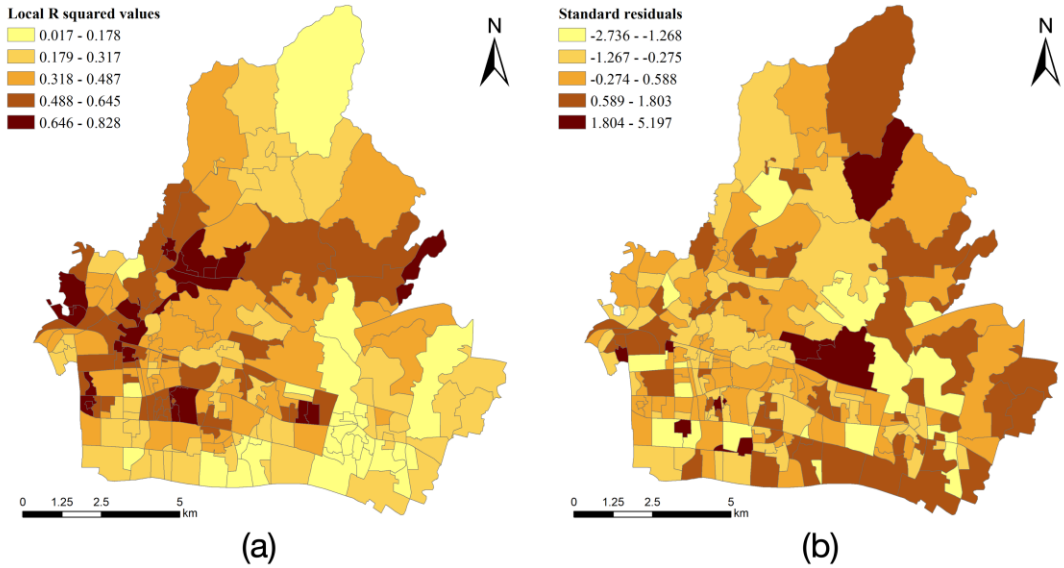

Figure 10. GWR statistical results. (a) Local R-squared values; (b) standard residuals.

5. Discussion

5.1 Comparing Top-down- and Human Perception-based Landscapes

Top-down-based landscapes are usually depicted from satellite and airborne remote sensing images including radiometer, radar and light detection and ranging (LiDAR) sensor images. Remote sensing views from the top-down perspective highly promote large-scale monitoring. In contrast, the availability of street view images has enabled urban landscape sensing from the perspective of human perception. Compared with top-down landscapes, human perception-based landscapes depict distinguishable urban environments from a perspective similar to that of human vision.

When top-down- and human perception-based views depict urban structures at the same location, the landscapes from different perspectives can be notably different. Figure 11 shows several examples of the spatial distributions of top-down- and human perception-based greenery in the study area. In area #1, continuous large-scale

greenery can be observed from the top-down perspective in Figure 11(b). The human perception-based greenery in this area exhibits similar patterns, as shown in Figure 11(a), where high IDW values occur. However, the spatial distributions of the top-down- and human perception-based greenery in area #1 are not consistent, namely, the greenery objects in the northern part of area #1 are clustered, whereas the human-perceived greenery objects are located in the central and southern areas. From this point of view, the differences in greenery between areas #2 and #3 can be determined. Specifically, Figure 11(a) shows peak IDW values in area #2 indicating much greenery, while in Figure 11(b), no significant greenery is identified in the top-down view. Another situation is depicted for area #3: although continuous greenery can be identified from a top-down perspective in the northern part, human-perceived greenery is lacking in this area.

From the above discussion, one can conclude that the spatial distributions of the top-down- and human perception-based greenery are not consistent. On the one hand, more human-perceived greenery was identified in certain regions compared with top-down sensing, while on the other hand, continuous large-scale greenery from the top-down perspective cannot be completely perceived by humans. As a result, the hypothesis that urban landscapes vary according to the different perspectives is proven.

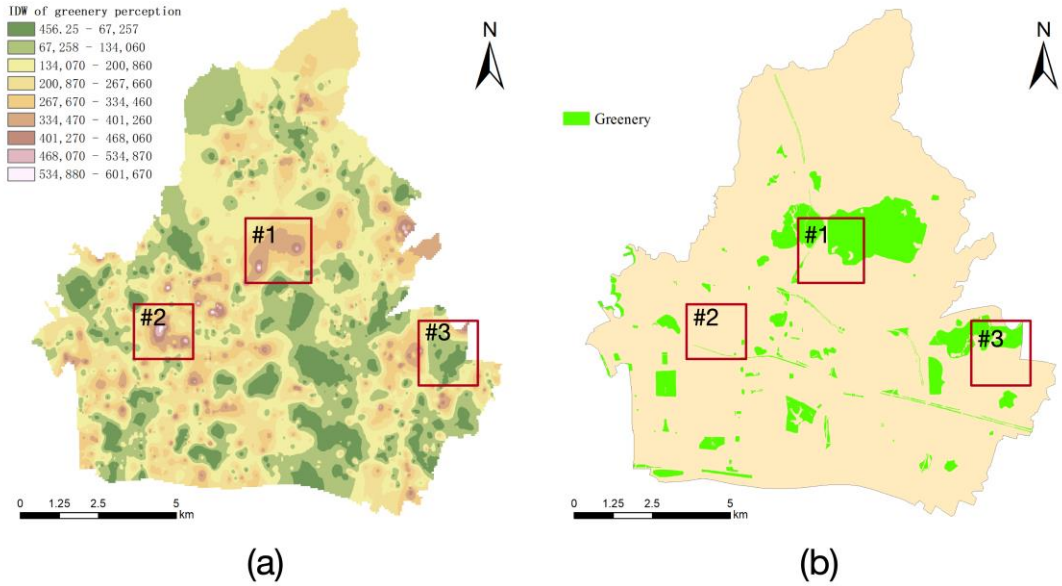

Figure 11. Human perception- and top-down-based greenery. (a) Human perception-based greenery; (b) top-down-based greenery.

5.2 Towards Human Perception-based Landscapes and Urban Poverty

As suggested in Figure 9, in most areas, percentage of green perception and aggregation of open space perception are negatively related to urban poverty, whereas percentage of open space perception and aggregation of greenery perception are positively correlated to urban poverty. The findings show the differences between

landscape occupation and inequality, that is the occupations of landscapes are not always consistent with the aggregation patterns.

To further distinguish occupation and inequality of human-perception-based landscape, "Positive/Negative- Positive/Negative" patterns are proposed, which means the positive/negative correlations between greenery-open space and urban poverty. Greenery occupation and inequality show opposite trends in northeast areas, indicating that different greenery characteristics show various impacts on urban poverty (see Figure 12(a)). Similar situation can be found in open space landscapes, in which opposite trends of occupation and inequality are shown in north and central regions (see Figure 12(b)).

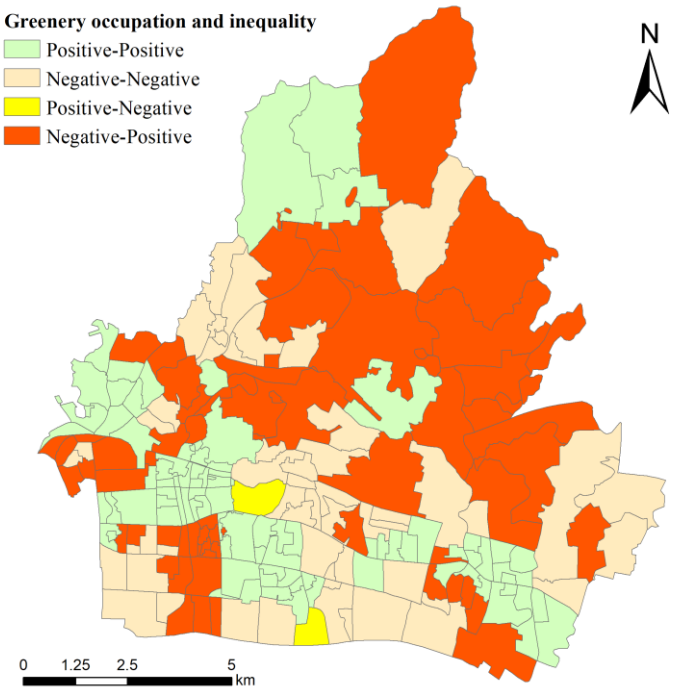

(a)

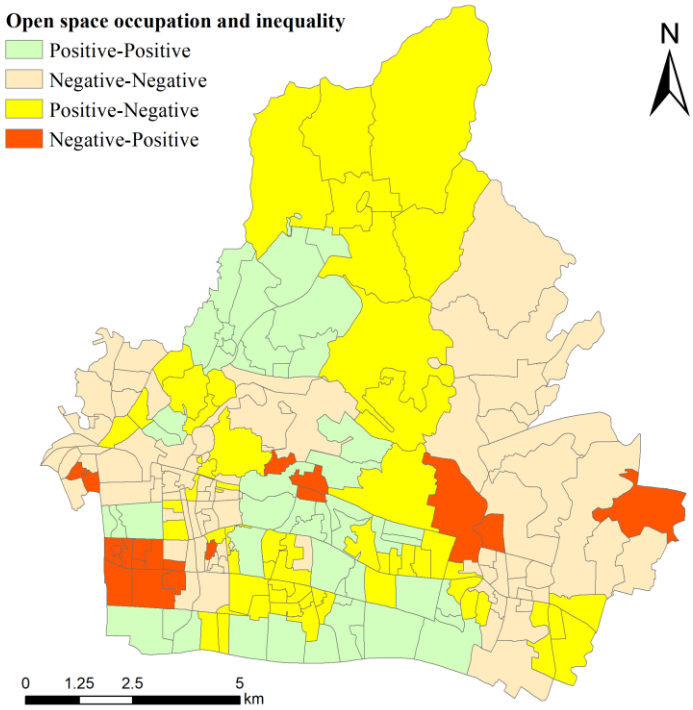

(b)

Figure 12. Differences of occupation and inequality in response to urban poverty. (a) Greenery occupation and inequality; (b) Open space occupation and inequality.

6. Conclusion

This study investigates greenery and open spaces from the perspective of occupation and inequality using street view images and further examines their relationship with urban poverty. To estimate the occupation and inequality between human perception-based greenery and open spaces, street view image segmentation and the IDW approach are applied, and four indicators, including greenery and open-space perception percentages and aggregations, are proposed. On this basis, GWR is utilised to analyse the relationship between human perception-based greenery and open-space landscapes and urban poverty.

With Tianhe District in Guangzhou as the study area, the results reveal that the greenery and open-space perception occupations vary among the different areas, while the inequalities increase from southwest to northeast. With an R-squared value of 0.667 for the GWR model, greenery and open spaces are highly related to urban poverty. In most areas, percentage of greenery perception is negatively related to urban poverty, while percentage of open space perception is positively correlated. But the aggregations of greenery and open space perceptions show opposite trends with positive and negative correlations, respectively.

References

Alkire, S., Santos, M. E., 2010, Acute multidimensional poverty: A new index for developing countries, *United Nations development programme human development report office background paper* (2010/11).

Bartier, P. M., Keller, C. P., 1996, Multivariate interpolation to incorporate thematic surface data using inverse distance weighting (IDW), *Computers & Geosciences* **22**(7)**:**795-799.

Brunsdon, C., Fotheringham, A. S., Charlton, M. E., 1996, Geographically weighted regression: a method for exploring spatial nonstationarity, *Geographical analysis* **28**(4)**:**281-298.

Chen, F. W., 2012, Estimation of the spatial rainfall distribution using inverse distance weighting (IDW) in the middle of Taiwan, *Paddy & Water Environment* **10**(3)**:**209-222.

Chen, J., Li, Z., 2018, China tracks its progress on SDGs, in: *Nature*, pp. 184.

Chen, Z., Xu, B., Devereux, B., 2014, Urban landscape pattern analysis based on 3D landscape models, *Applied Geography* **55:**82-91.

Elvidge, C. D., Sutton, P. C., Ghosh, T., Tuttle, B. T., Baugh, K. E., Bhaduri, B., Bright, E., 2009, A global poverty map derived from satellite data, *Computers & Geosciences* **35**(8)**:**1652-1660.

He, H. S., Dezonia, B. E., Mladenoff, D. J., 2000, An aggregation index (AI) to quantify spatial patterns of landscapes, *Landscape Ecology* **15**(7)**:**591-601.

Helbich, M., Yao, Y., Liu, Y., Zhang, J., Liu, P., Wang, R., 2019, Using deep learning to examine street view green and blue spaces and their associations with geriatric depression in Beijing, China, *Environment international* **126:**107-117.

Ho, H. C., Wong, M. S., Man, H. Y., Shi, Y., Abbas, S., 2019, Neighborhood-based subjective environmental vulnerability index for community health assessment: Development, validation and evaluation, *Science of The Total Environment* **654:**1082-1090.

Jim, C. Y., Chen, W. Y., 2008, Assessing the ecosystem service of air pollutant removal by urban trees in Guangzhou (China), *Journal of environmental management* **88**(4)**:**665-676.

Kabisch, N., Haase, D., 2014, Green justice or just green? Provision of urban green spaces in Berlin, Germany, *Landscape and Urban Planning* **122:**129-139.

Klasen, S., 2000, Measuring poverty and deprivation in South Africa, *Review of income and wealth* **46**(1)**:**33-58.

Knox, P., Pinch, S., 2014, Urban social geography: an introduction, Routledge.

Langlois, A., Kitchen, P., 2001, Identifying and measuring dimensions of urban deprivation in Montreal: An analysis of the 1996 census data, *Urban Studies* **38**(1)**:**119-139.

Lee, A. C., Maheswaran, R., 2011, The health benefits of urban green spaces: a review of the evidence, *Journal of public health* **33**(2)**:**212-222.

Li, X., Zhang, C., Li, W., Kuzovkina, Y. A., Weiner, D., 2015, Who lives in greener neighborhoods? The distribution of street greenery and its association with residents' socioeconomic conditions in Hartford, Connecticut, USA, *Urban Forestry & Urban Greening* **14**(4)**:**751-759.

Li, Z., Wei, H., Wu, Y., Su, S., Wang, W., Qu, C., 2019, Impact of community deprivation on urban park access over time: Understanding the relative role of contributors for urban planning, *Habitat International***:**102031.

Liu, M., Hu, Y.-M., Li, C.-L., 2017, Landscape metrics for three-dimensional urban building pattern recognition, *Applied Geography* **87:**66-72.
Liu, R., Kuffer, M., Persello, C., 2019, The Temporal Dynamics of Slums Employing a CNN-Based Change Detection Approach, *Remote Sensing* **11**(23)**:**2844.
Noble, M., Barnes, H., Wright, G., Roberts, B., 2010, Small area indices of multiple deprivation in South Africa, *Social indicators research* **95**(2)**:**281.
Oke, T. R., 2002, Boundary layer climates, Routledge.
Schroeder, H. W., Cannon, W., 1983, The esthetic contribution of trees to residential streets in Ohio towns, *Journal of Arboriculture* **9**(9)**:**237-243.
Stubbings, P., Peskett, J., Rowe, F., Arribas-Bel, D., 2019, A Hierarchical Urban Forest Index Using Street-Level Imagery and Deep Learning, *Remote Sensing* **11**(12)**:**1395.
Tang, J., Long, Y., 2018, Measuring visual quality of street space and its temporal variation: Methodology and its application in the Hutong area in Beijing, *Landscape and Urban Planning*.
Wang, J., Kuffer, M., Roy, D., Pfeffer, K., 2019a, Deprivation pockets through the lens of convolutional neural networks, *Remote sensing of environment* **234:**111448.
Wang, R., Liu, Y., Lu, Y., Zhang, J., Liu, P., Yao, Y., Grekousis, G., 2019b, Perceptions of built environment and health outcomes for older Chinese in Beijing: A big data approach with street view images and deep learning technique, *Computers, Environment and Urban Systems* **78:**101386.
Weng, Q., Lu, D., Schubring, J., 2004, Estimation of land surface temperature–vegetation abundance relationship for urban heat island studies, *Remote sensing of Environment* **89**(4)**:**467-483.
Wolfe, M. K., Mennis, J., 2012, Does vegetation encourage or suppress urban crime? Evidence from Philadelphia, PA, *Landscape and Urban Planning* **108**(2-4)**:**112-122.
Xing, H., Meng, Y., 2018, Integrating landscape metrics and socioeconomic features for urban functional region classification, *Computers, Environment and Urban Systems* **72:**134-145.
Yin, L., Wang, Z., 2016, Measuring visual enclosure for street walkability: Using machine learning algorithms and Google Street View imagery, *Applied Geography* **76:**147-153.
Yuan, Y., Wu, F., 2014, The development of the index of multiple deprivations from small-area population census in the city of Guangzhou, PRC, *Habitat International* **41:**142-149.
Yuen, J. W., Chang, K. K., Wong, F. K., Wong, F. Y., Siu, J. Y., Ho, H., Wong, M., Ho, J., Chan, K., Yang, L., 2019, Influence of Urban Green Space and Facility Accessibility on Exercise and Healthy Diet in Hong Kong, *International journal of environmental research and public health* **16**(9)**:**1514.
Zhang, F., Zhang, D., Liu, Y., Lin, H., 2018, Representing place locales using scene elements, *Computers, Environment and Urban Systems* **71:**153-164.
Zhao, H., Shi, J., Qi, X., Wang, X., Jia, J., 2017, Pyramid scene parsing network, in: *Proceedings of the IEEE conference on computer vision and pattern recognition*, pp. 2881-2890.
Zhou, B., Zhao, H., Puig, X., Fidler, S., Barriuso, A., Torralba, A., 2017, Scene parsing through ade20k dataset, in: *Proceedings of the IEEE conference on computer vision and pattern recognition*, pp. 633-641.
Zhu, R., Wong, M. S., Guilbert, É., Chan, P.-W., 2017, Understanding heat patterns produced by vehicular flows in urban areas, *Scientific reports* **7**(1)**:**16309.

Zimmerman, D., Pavlik, C., Ruggles, A., Armstrong, M. P., 1999, An Experimental Comparison of Ordinary and Universal Kriging and Inverse Distance Weighting, *Mathematical Geology* **31**(4)**:**375-390.